Afyon Kocatepe Üniversitesi Fen ve Mühendislik Bilimleri Dergisi
Afyon Kocatepe University – Journal of Science and Engineering
https://dergipark.org.tr/tr/pub/akufemubid

Araştırma Makalesi / Research Article
e-ISSN: 2149-3367
DOI: https://doi.org/10.35414/akufemubid.1625167
AKÜ FEMÜBİD **25** (2025) 055802 (1193-1201)
AKU J. Sci. Eng. **25** (2025) 055802 (1193-1201)

May 2024 Gannon Superstorm: Insights from Ground-based Magnetometer Measurements

Makale Bilgisi / Article Info
Alındı/Received: 22.01.2025
Kabul/Accepted: 03.04.2025
Yayımlandı/Published: 01.10.2025

Mayıs 2024 Gannon Süperfırtınası: Yer Tabanlı Manyetometre Ölçümlerinden Elde Edilen Bulgular

Özlem HACIOĞLU[1*], Elif ÇİFTÇİ[2]

[1] *Karadeniz Technical University, Faculty of Engineering, Department of Geophysical Engineering, Trabzon, Türkiye*
[2] *Boğaziçi University, Kandilli Observatory and Earthquake Research Institute, Department of Geophysics, İstanbul, Türkiye*

© 2025 The Authors | Creative Commons Attribution-Noncommercial 4.0 (CC BY-NC) International License

Abstract

On May 10–11, 2024, one of the strongest geomagnetic storms in recent years swept across the planet. Several interplanetary coronal mass ejections (ICMEs) originated from the source active region (AR 13664), propelling solar energetic particles toward Earth. Triggered by intense solar eruptions, the storm reached a Kp index of 9 (the highest on the scale), causing a remarkable expansion of auroras visible far beyond their usual high latitudes. The unprecedented strength of the storm highlights the necessity of monitoring geomagnetic disturbances using ground-based instruments to assess the far-reaching impacts of space weather events, especially in regions well beyond the typical auroral zones. In this study, geomagnetic data from several observatories located in mid-latitudes (30°-60°N) in the Northern Hemisphere were therefore utilized to analyze the G5-level super-intense Gannon storm. These observations enable the detection of geomagnetic variations, including sudden storm commencements (SSCs), prolonged negative excursions in the Disturbance Storm-Time (Dst) index, as well as localized magnetic fluctuations indicative of intensified ionospheric currents. Additionally, the auroral electrojet strength and the asymmetric distribution of geomagnetic disturbances provide critical insights into the spatial and temporal evolution of ionospheric and magnetospheric processes during the extreme geomagnetic storm, helping to understand its impacts on mid-latitude regions. The results highlight the spatial variability and temporal synchronicity of the impacts of the storm, demonstrating the crucial role of mid-latitude observatories in capturing ionospheric and magnetospheric responses during extreme geomagnetic events.

Keywords: Space Weather; Geomagnetic Storms; Geomagnetic Field; Geophysics

Öz

10-11 Mayıs 2024 tarihlerinde, son yılların en güçlü jeomanyetik fırtınalarından biri dünya genelinde etkili olmuştur. Kaynak aktif bölge (AR 13664) kaynaklı gezegenler arası koronal kütle atımları (ICME), güneş enerjili parçacıkları Dünya'ya yönlendirmiştir. Yoğun güneş patlamalarının tetiklediği bu fırtına, Kp indeksinde 9 seviyesine ulaşmış (ölçekteki en yüksek seviye) ve olağan yüksek enlemlerin çok ötesinde görülebilen aurora genişlemelerine neden olmuştur. Fırtınanın benzeri görülmemiş gücü, özellikle tipik aurora bölgelerinin çok ötesindeki bölgelerde uzay hava olaylarının geniş kapsamlı etkilerini değerlendirmek için yer tabanlı ekipmanlarla jeomanyetik rahatsızlıkların izlenmesinin gerekliliğini vurgulamaktadır. Bu çalışmada, Kuzey Yarımküre'de orta enlemlerde (30°-60°K) bulunan birkaç gözlemevinden elde edilen jeomanyetik veriler, G5 seviyesindeki Gannon fırtınasını analiz etmek için kullanılmıştır. Bu gözlemler, ani fırtına başlangıçları (SSC'ler), Bozulma Fırtına-Zaman (Dst) indeksindeki uzun süreli negatif sapmalar ve yoğunlaşmış iyonosferik akımları gösteren yerel manyetik dalgalanmalar dahil olmak üzere jeomanyetik değişimlerin tespit edilmesini sağlamaktadır. Ayrıca, auroral elektrojet gücü ve jeomanyetik bozuklukların asimetrik dağılımı, güçlü jeomanyetik fırtına sırasında iyonosferik ve manyetosferik süreçlerin mekansal ve zamansal evrimine ilişkin önemli bilgiler sunmaktadır. Bu bulgular, fırtınanın etkilerinin mekansal değişkenliğini ve zamansal eşzamanlılığını vurgulamakta ve orta enlem gözlemevlerinin aşırı jeomanyetik olaylar sırasında iyonosferik ve manyetosferik tepkileri yakalamadaki kritik rolünü göstermektedir.

Anahtar Kelimeler: Uzay Havası; Jeomanyetik Fırtınalar; Jeomanyetik Alan; Jeofizik

1. Introduction

Geomagnetic storms are significant disturbances in the Earth's magnetosphere caused primarily by interplanetary coronal mass ejections (ICMEs) and high-speed solar wind streams interacting with the Earth's magnetic field (e.g., Gosling *et al.* 1990, Schwenn, 2006, Gonzalez *et al.* 2007, Watari, 2017). These interactions can lead to complex geomagnetic disturbances observable on a planetary scale, especially in the auroral regions.

ICMEs, originating from active regions of the Sun, are frequently associated with sudden increases in solar wind density and magnetic field intensity. When these structures reach the Earth's magnetosphere, they can

*Sorumlu Yazar/Corresponding Author: Özlem HACIOĞLU e-posta/e-mail: ozlem.hacioglu@ktu.edu.tr

trigger phenomena such as the Sudden Storm Commencements (SSCs) and prolonged depressions in the Disturbance Storm Time (Dst) index, indicative of severe magnetic reconnection events (e.g., Kwak *et al.* 2024, Spogli *et al.* 2024). Furthermore, variations in the asymmetric horizontal component and the declination of the Earth magnetic field provide additional insights into substorm activity and the dynamics of current systems (e.g., Wu *et al.* 2008, Gillies *et al.* 2012). During ICME impacts, enhanced asymmetries in the magnetic field can reflect the intensification of auroral electrojets and shifts in magnetospheric symmetry, suggesting a more detailed perspective on the distribution of geomagnetic disturbances (e.g., Dubyagin *et al.* 2014, Makarov 2022, Collado- Villaverde 2024).

One of the most notable geomagnetic storms of the last two decades occurred during the Halloween Storm of 2003, which served as a benchmark for understanding the impacts of such events at both high and mid-latitudes (e.g., Baker *et al.* 2004). The most intense event since the Halloween Storm, the geomagnetic storm of May 10–11, 2024, known as the Gannon Storm (initially referred to as the Mother's Day Storm but later renamed Gannon in memory of Dr. Jennifer Gannon) (e.g., Tulasi Ram *et al.* 2024, Kwak *et al.* 2024, Singh *et al.* 2024, Foster *et al.* 2024), stands out due to a series of X-class solar flares (Table 1) from the active region AR 13664 (Figure 1) and the strength of the ICMEs it generated.

With a Kp index peaking at 9, this event caused auroras visible at latitudes as low as 30°N, even reaching as far south as 21°N, highlighting the global impact of the storm and the importance of mid- and low-latitude observatories in capturing geomagnetic anomalies, particularly during storms of G5 intensity levels (e.g., Grandin *et al.* 2024, Parker and Linares 2024, Spogli *et al.* 2024).

Table 1: X-class solar flare events were generated in active region (AR) 13664, with their peak, start and end times, GOES class, and source location identified by the National Oceanic and Atmospheric Administration (NOAA).

Date	Start time (UT)	Peak time (UT)	End time (UT)	GOES Class	Derived Position
2024/05/08	21:08:00	21:40:00	21:58:17	X1.0	S20W17
2024/05/09	08:45:00	09:13:00	09:31:20	X2.3	S20W24
2024/05/09	17:23:00	17:44:00	18:01:19	X1.1	S17W28
2024/05/10	06:27:00	06:54:00	07:13:19	X4.0	S17W34
2024/05/11	11:15:00	11:44:00	12:01:20	X1.5	S19W60
2024/05/11	01:10:00	01:23:00	01:39:00	X5.8	S17W44
2024/05/12	16:11:00	16:26:00	16:43:24	X1.0	S20W75
2024/05/14	16:46:00	16:51:00	17:02:00	X8.7	S18W89
2024/05/14	12:40:00	12:55:00	13:05:00	X1.2	S17W89
2024/05/14	02:03:00	02:09:00	02:19:00	X1.7	S17W89
2024/05/15	08:18:00	08:37:00	08:55:34	X3.5	S18W89

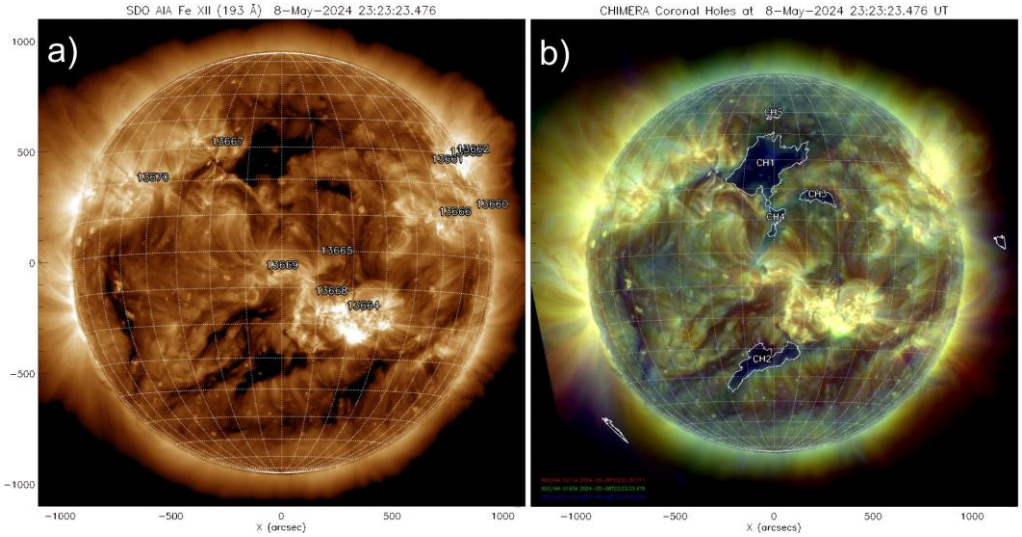


Figure 1. a) The Solar Dynamics Observatory (SDO) AIA image shows the source active regions, particularly AR 13664 the source of the intense geomagnetic activity that led to the May 10–11, 2024, Gannon Storm, associated with the solar flares on May, 2024. These active regions are labeled with their respective NOAA numbers. b) A map of coronal holes (CHs) showing regions where the Sun's magnetic field lines extend outward into space. These coronal holes contribute to the enhanced solar wind streams interacting with interplanetary coronal mass ejections (ICMEs). The image captures solar conditions preceding the Gannon Storm, which featured multiple X-class solar flares and exceptionally strong ICME dynamics.

Understanding such rare G5-level geomagnetic storms requires comprehensive data from ground-based magnetometers, which allow researchers to observe localized magnetic field variations and identify intensified ionospheric currents. This study aims to analyze the propagation and characteristics of the May 2024 geomagnetic storm, obtaining data from mid-latitude observatories across Europe. The study also seeks to elucidate the dynamics of geomagnetic disturbances and the significance of mid-latitude monitoring stations in space weather research.

2. Data and Method

The magnetic response of the Earth to solar activity, including intense bursts of energy and radiation from the Sun, is monitored through a global network of ground-based magnetometers. These stations continuously record variations in the geomagnetic field in the form of time-series data, offering critical data for identifying patterns and anomalies in geomagnetic activity and enhancing space weather predictions.

Magnetic observatories across the globe continuously monitor the magnetic field of the Earth by measuring its vector components, facilitating analysis of geomagnetic activity. At each observatory, the three vector components (X, Y, and Z) or, alternatively, the magnetic elements (H, D, and Z) in various configurations are recorded at intervals of one second or one minute. The horizontal component, H, is calculated from the northward (X) and eastward (Y) components using the formula $H = \sqrt{X^2 + Y^2}$. In this study, the horizontal component of the geomagnetic field was obtained from observatory magnetometers participating in INTERMAGNET (International Real-time Magnetic Observatory Network). The disturbance in H component at each station is determined by subtracting the H component variation recorded on a reference quiet day (9 May 2024) from the variations observed during the storm days (10 and 11 May 2024) at the corresponding stations. Figure 2 illustrates the geographical distribution of these stations across Europe, where mid-latitude auroras were recorded during the recent Gannon storm of May 10–11, 2024 (e.g., Grandin *et al.* 2024).

The International Geomagnetic Reference Field (IGRF), calculated using spherical harmonic components for total field intensity, was also plotted on the map. Table 2 provides details of each observatory, including their geomagnetic and geographic coordinates and their IAGA (International Association of Geomagnetism and Aeronomy) codes. Moreover, for each magnetic component of each observatory, we have calculated the differences of the momentary values by subtracting each participating observatory momentary value from the respective IZN value:

$$\Delta a = a_{IZN} - a_{XXX}$$

where a_{IZN} and a_{XXX} are the momentary values for a magnetic element and XXX stands for the three letter IAGA code of a magnetic observatory. For comparison, the values have been normalized using an artificial offset to ensure they start from a common reference point, as described by Curto and Marshal (2007). We chose IZN as a reference observatory since auroras are typically observed down to about 40°.

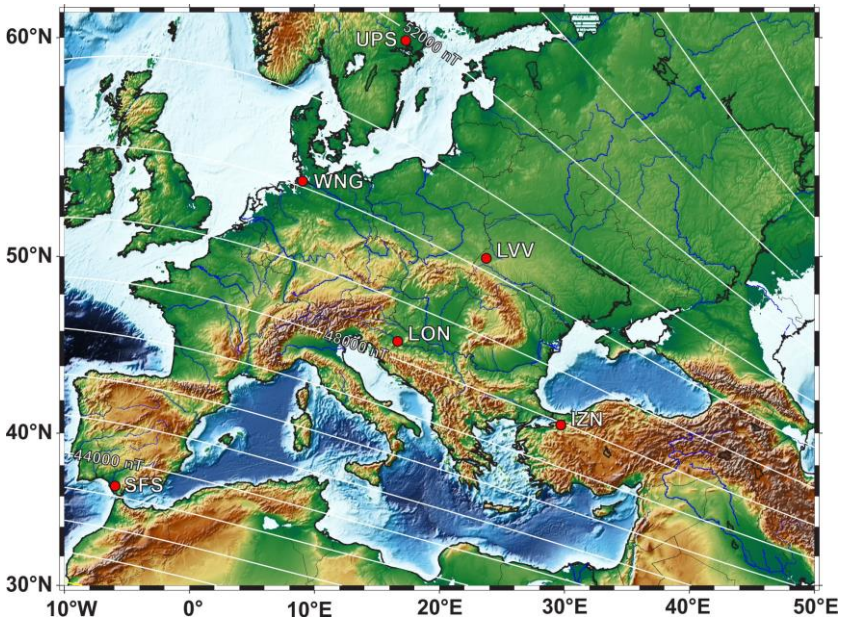


Figure 2. The map shows the locations of mid-latitude geomagnetic observatories (UPS, WNG, LVV, LON, IZN, and SFS) across Europe, from which magnetic data were obtained and analyzed. The magnetic intensity contours, based on the IGRF model, illustrate variations in Earth's magnetic field strength across the region.

Table 2. Geomagnetic observatories identified by their location and IAGA codes.

Observatory	Geographic Latitude (deg)	Geographic Longitude (deg)	Geomagnetic Latitude (deg)	Geomagnetic Longitude (deg)
Uppsala (UPS)	59.903	17.353	56.57	94.42
Wingst (WNG)	53.725	9.053	49.79	85.77
Lviv (LVV)	49.90	23.75	45.5	97.54
Lonjsko Polje (LON)	45.408	16.659	40.24	90.92
Istanbul (IZN)	40.50	29.72	35.35	102.63
San Fernando (SFS)	36.667	354.055	26.66	69.6

Geomagnetic indices Kp, Dst and its higher temporal resolution Sym-H (symmetric disturbance index, 1 minute interval), AE, Asy (asymmetric disturbance index), and ap/Hp30 were utilized to characterize variations in the magnetic field of the Earth during the Gannon superstorm. The strength of geomagnetic storms is commonly classified using the 3-hour Kp index, with levels 8 and 9 indicating extreme events on a 0–9 scale. The Kp index measures global geomagnetic activity and represents a weighted average of K indices from 13 subauroral (i.e., geomagnetic latitudes between 44° and 60°) observatories located in both the Northern and Southern Hemispheres (Bartels *et al.* 1939). It is sensitive to the equatorward extent of the auroral oval, reflecting the intensity of magnetospheric convection (Thomsen 2004). The Dst index, derived from the horizontal component of the Earth's magnetic field measured by a network of low-latitude ground-based magnetometers, provides continuous data on the Earth's magnetic field (Lakhina and Tsurutani, 2016) and is attributed to the strength of the magnetospheric ring currents (Daglis 2006). The AE (Auroral Electrojet) index, based on measurements from a network of high latitude ground-based magnetometers around the auroral zone, is used to quantify the intensity of the auroral electrojets, which are intense electric currents flowing in the ionosphere at high latitudes (e.g., Akasofu 1981). The Asy index, derived from measurements at a network of low- and mid-latitude geomagnetic observatories, is used to measure the asymmetry in the Earth's geomagnetic field caused by currents that occur during geomagnetic storms (e.g., Singh *et al.* 2012). The recent high-resolution geomagnetic indices, ap/Hp-30, are also calculated in the same way as Kp. However, unlike Kp, the Hpo index does not have an upper limit of 9, enabling to quantify severe geomagnetic storms without limitations (Yamazaki *et al.* 2022, 2024). The Kp, Hpo, and ap30 indices, characterizing the variation of geomagnetic activity were obtained from the ISGI (International Service of Geomagnetic Indices), in collaboration with the GFZ German Research Centre for Geosciences. The Dst, AE, Asy H/D and Sym-H indices was provided by the WDC (World Data Centre for Geomagnetism), Kyoto, Japan. The real-time Dst was derived from preliminary raw data due to the final Dst data not being available yet. To implement the developed network, the real-time solar wind and interplanetary magnetic field data were obtained from the OMNI (NASA's Space Physics Data Facility).

3. Results and Discussions

The recent Gannon storm of May 10–11, 2024, a significant event in the ongoing 25th solar cycle, resulted from an enhanced transfer of solar wind energy into the ionosphere-thermosphere, leading to the global observation of auroras. Figure 3 presents an overview of the interplanetary magnetic field (IMF) and plasma parameters associated with the May 10–11, 2024, geomagnetic storm, providing critical insights into the initiation and progression of the Gannon storm.

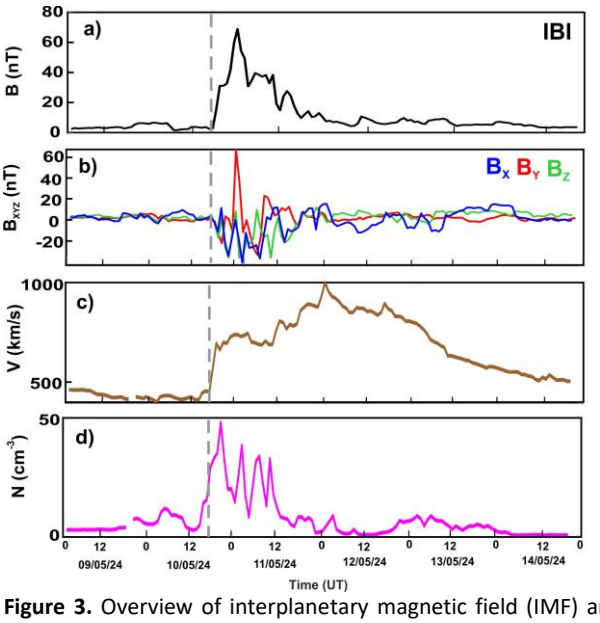


Figure 3. Overview of interplanetary magnetic field (IMF) and plasma parameters during the May 10–11, 2024, Gannon Storm. (a) Total magnetic field strength (B). (b) IMF components (Bx, By, Bz). (c) Solar wind speed (V). (d) Solar wind density (N). The dashed gray line marks the storm's sudden commencement (SSC).

The abrupt increase in the total magnetic field B, from a few nT around 16:00 UT on May 10, 2024, to a maximum of 69 nT at 23:00 UT, indicates the arrival of the

interplanetary coronal mass ejection (ICME), marked by a sharp peak near the SSC (dashed gray line) (Figure 3a). The Bx, By and Bz components of the IMF, with the southward (i.e., negative) turning of Bz (max. magnitude -35 nT at around 21:00 UT on 10 May, 00:00 UT on 11 May, and 09:00 UT on 11 May) evident during the most intense phase of the storm, a key driver of geomagnetic reconnection and the injection of charged particles into the magnetosphere (Figure 3b). The solar wind speed V, showing a sharp rise to values following IMF strength from about 400 km/s to over 700 km/s and exceeding 1000 km/s at 01:00 UT on 12 May, after which it gradually decays, characteristic of high-speed plasma ejections (Figure 3c). The gap in the data during the earliest hours arises from missing measurements. The solar wind (i.e., proton) density N also shows significant fluctuations, reaching a maximum of 53 cm^3 at 20:00 UT on 10 May, concurrent with the shock arrival and subsequent ICME phases (Figure 3d). The decay on density around 12:00 UT on May 11 is consistent with the decay on the IMF but the flow speed remains high (Figure 3a and b). These enhancements in velocity and density demonstrate the dynamic compression of the magnetosphere, which leads to geomagnetic disturbances.

Figure 4 illustrates the global and regional geomagnetic impacts of the May 10–11, 2024, Gannon storm, combining the Kp and Dst indices with the variations in the horizontal component ΔH of the magnetic field from mid-latitude observatories. The uppermost panel shows the Kp index alongside the Dst index, illustrating the rapid decline associated with the sudden storm commencement (SSC) and subsequent intensification of geomagnetic activity. The Kp index peaked at around 9 at 21:00 UT on 10 May 2024, as well as at 9 at 00:00 UT and 09:00 UT on 11 May 2024, indicating an extreme G5-level geomagnetic storm according to the NOAA Space Weather Scales. Additionally, the Dst index, which reached its minimum value of -412 nT at 03:00 UT on 11 May 2024, dropped sharply below -200 nT, reflecting intense ring current enhancement. The subsequent panels also exhibit the geomagnetic responses at mid-latitude stations (UPS, WNG, LVV, LON, IZN, and SFS), revealing localized differences in ΔH.

Each observatory exhibits pronounced variations in the magnetic field, demonstrating the synchronous impact of the ICME arrival. Regional differences are evident, with UPS experiencing the largest disturbances and SFS recording the lowest values due to latitude variations, highlighting the spatial variability of ionospheric and magnetospheric currents. Additionally, the fluctuations of ΔH across stations indicates the development of strong ionospheric currents and variations in the intensity of auroral electrojets. The alignment between ΔH and Sym-H index (max. ~518 nT) trends highlights the coupling between global ring current dynamics and localized geomagnetic responses, demonstrating the importance of mid-latitude stations in capturing the widespread effects of the storm and the critical role of mid-latitude observatories in capturing the dynamics of geomagnetic disturbances, particularly during the expansion phase of the auroral oval.

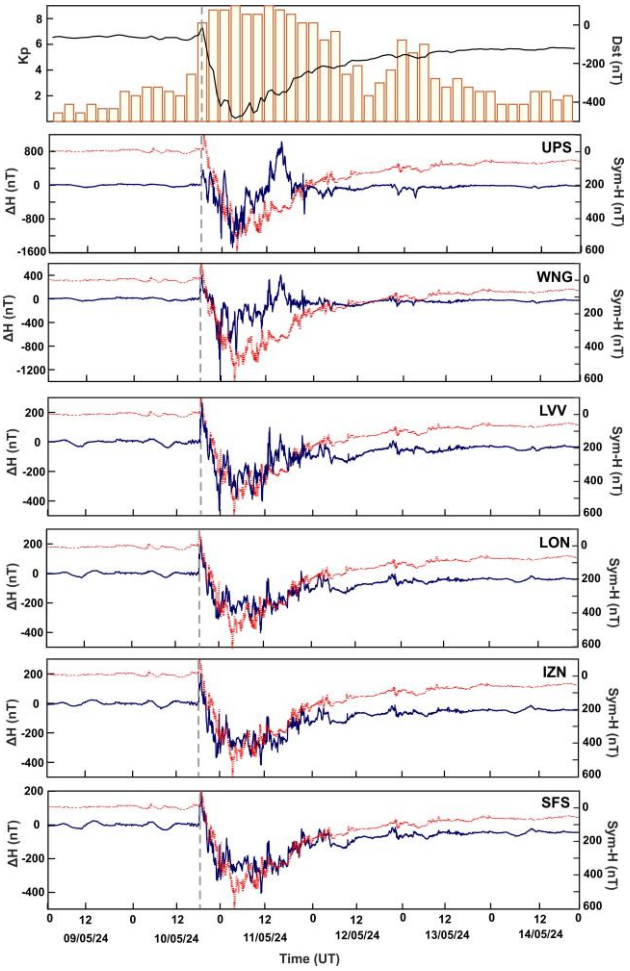


Figure 4. The global and regional geomagnetic impacts of the May 10–11, 2024, Gannon Storm are shown. The top panel illustrates the Kp (bars) and Dst (black) indices, while the lower panels display the horizontal magnetic field component (ΔH) (blue) and the Sym-H index (red) at mid-latitude observatories (UPS, WNG, LVV, LON, IZN, SFS), highlighting pronounced geomagnetic variations caused by the ICME arrival.

The spatial variability of geomagnetic disturbances during the May 10–11, 2024 Gannon storm, showing the differences in the magnetic components (H, Z, D, F) between the IZN reference station and other mid-latitude observatories are shown in Figure 5. The horizontal component (H) displays pronounced negative excursions at the onset of the storm, particularly at UPS and WNG, indicating enhanced ionospheric currents and a strong westward electrojet (Figure 5a).

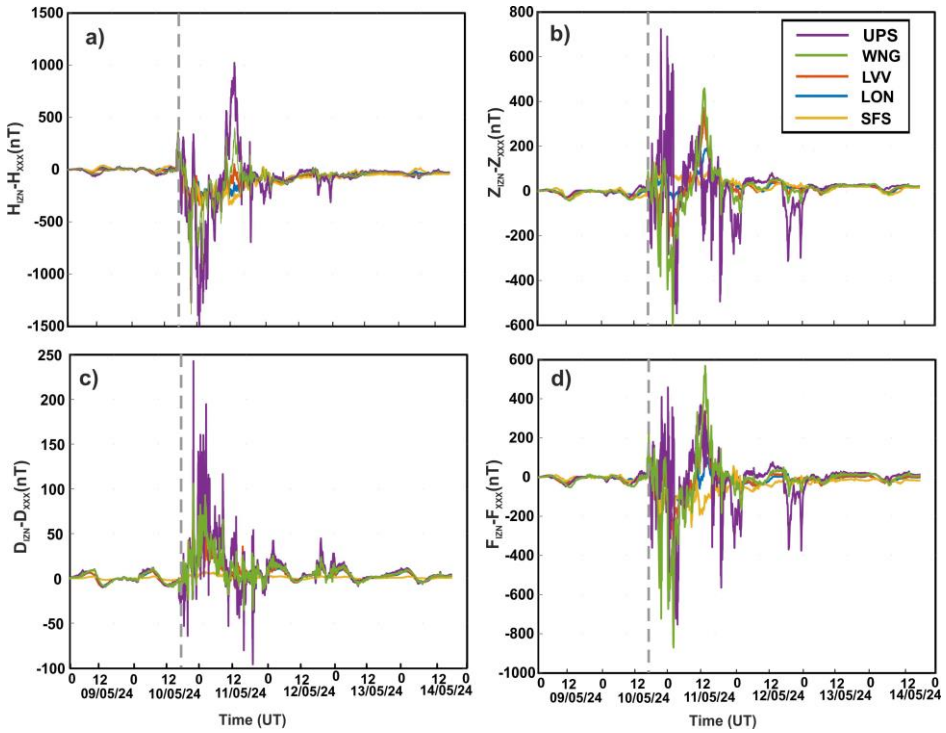
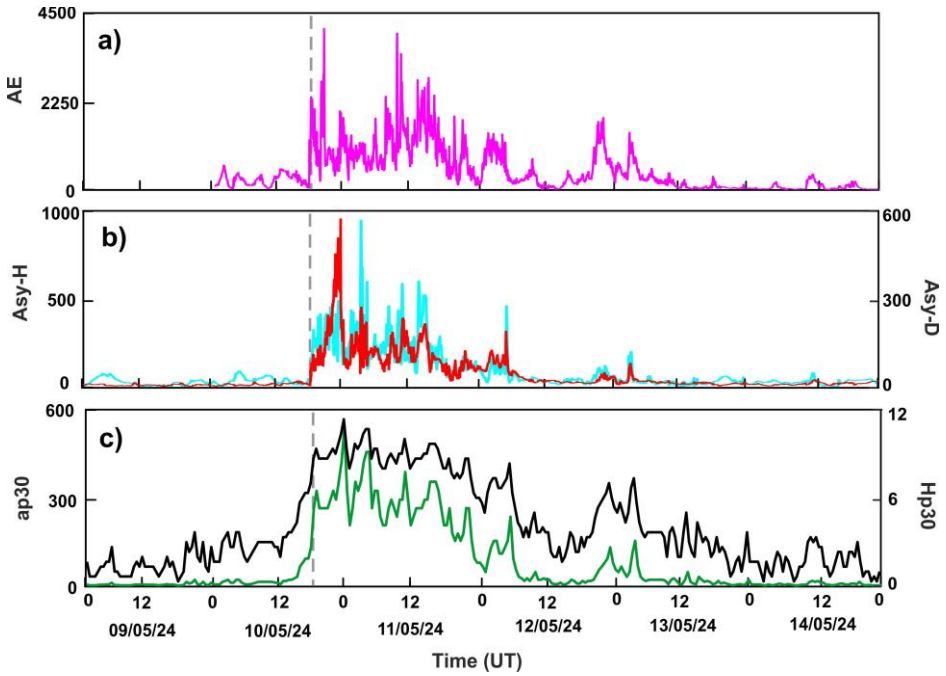


Figure 5. Spatial variability of geomagnetic disturbances during the May 10–11, 2024, Gannon Storm, showing differences in magnetic components (H, Z, D, F) between the IZN reference station and other mid-latitude observatories. (a) The horizontal component (H). (b) The vertical component (Z). (c) The declination (D). (d) The total field intensity (F).

The vertical component (Z) shows sharp fluctuations, reflecting significant field-aligned current systems and asymmetry in the magnetospheric compression (Figure 5b). The declination (D), demonstrates noticeable lateral shifts in the magnetic field, with larger variations observed at UPS, suggesting localized azimuthal distortions (Figure 5c). The total field intensity (F) capture the compounded effects of all components, reflecting the overall impact of the geomagnetic disturbance (Figure 5d). Moreover, these observations illustrate the temporal synchronicity but spatial heterogeneity of the storm's impact, proposing the importance of multi-station analyses to capture the dynamics of extreme geomagnetic events and their ionospheric and magnetospheric effects across mid-latitude regions.



Şekil 6. Geomagnetic indices (AE, Asy-H/D, ap30, and Hp30) characterizing the intensity and asymmetry of geomagnetic disturbances during the May 10–11, 2024, Gannon Storm. (a) The Auroral Electrojet (AE) index. The gap on May 9, 2024, is due to missing measurements. (b) Asy-H (red) and Asy-D (blue) indices. (c) The ap30 (green) and Hp30 (black) indices.

The geomagnetic indices (AE, Asy-H/D and ap/Hp30) that characterize the intensity and asymmetry of the geomagnetic disturbances during the Gannon storm on May 10–11, 2024 are shown in Figure 6. A sharp increase in the Auroral Electrojet (AE) index that shows the strength of ionospheric currents at high latitudes, peaking 4098 nT at around 20:00, indicates substantial intensification of auroral electrojets and the extreme magnetospheric energy injection during the storm (Figure 6a). The asymmetry indices Asy-H (horizontal) and Asy-D (declination), which represent the degree of north-south and east-west asymmetry in geomagnetic disturbances are shown in Figure 6b. The substantial peaks, particularly in Asy-H, suggest significant variations in current systems and uneven magnetic reconnection events across different regions. The ap30 and Hp30 indices, providing high-resolution representations of global geomagnetic activity are also demonstrated in Figure 6c. The ap30 index rises sharply during the SSC and remains elevated throughout the storm, highlighting sustained geomagnetic unrest. The Hp30, with a maximum value exceeding 11 on 11 May 2024, which lacks the upper limit of the Kp scale (Yamazaki *et al.* 2024), captures the extreme levels of geomagnetic disturbance without saturation, further reflecting the unprecedented intensity of this event. The elevated Asy-H and AE indices emphasize the role of asymmetric ionospheric currents and auroral electrojets, while the prolonged ap30 activity confirms the global scale of the geomagnetic disturbance. These combined indices highlight the dynamic progression of the storm, from the sudden onset to the prolonged recovery phase, demonstrating the necessity of high temporal resolution data to fully capture the complex nature of G5-level geomagnetic storms.

4. Conclusions

The Gannon geomagnetic storm of May 10–11, 2024, stands out as one of the most intense space weather events of the 25th solar cycle, characterized by unprecedented global impacts and mid-latitude auroral displays. The analysis of geomagnetic data from mid-latitude observatories highlights the spatial variability of the storm and temporal evolution, with significant disturbances observed in H, Z, and D components of the magnetic field. The pronounced and abrupt shifts in the H components signify the occurrence of an SSC, followed by sustained negative excursions in the Dst index, which indicate prolonged magnetospheric compression and significant ring current intensification. The fluctuations in geomagnetic indices, such as AE, Asy-H/D, Hp30, also highlight the dynamic coupling between the magnetosphere and ionosphere, revealing the intensification of auroral electrojets and the redistribution of magnetospheric currents driven by interactions between the solar wind and the magnetic field of the Earth. The fluctuations in mid-latitude indices (i.e. Asy) coincided with peaks in the auroral electrojet (AE) index, illustrating the substantial intensification of ionospheric currents and their spatial expansion far beyond typical auroral zones. The high-resolution Sym-H and Hp30 indices captured the rapid onset and prolonged recovery phase of the storm, emphasizing the importance of continuous monitoring to assess the full impact of such extreme events. The observational data demonstrate that mid-latitude stations play a significant role in tracking the propagation of geomagnetic disturbances, as they offer valuable insights into the expansion of the auroral oval and the development of substorm activity beyond high-latitude regions.

By highlighting the notable spatial variability and asymmetries observed during the Gannon storm, the current study contributes to enhancing predictive models of space weather, thereby supporting efforts to reduce the negative effects on global technological infrastructure and communication systems.

Declaration of Ethical Standards

The authors declare that they comply with all ethical standards.

Credit Authorship Contribution Statement

Author-1: Conceptualization, methodology, investigation, software, visualization, writing and reviewing.

Author-2: Conceptualization, methodology, investigation, software, visualization, writing and reviewing.

Declaration of Competing Interest

The author declares no conflicts of interest.

Data Availability Statement

Datasets are available on request. The raw data supporting the conclusions of this article will be made available by the authors, without undue reservation.

Acknowledgement

The authors thank INTERMAGNET (International Real-time Magnetic Observatory Network) and the geomagnetic observatories proving the geomagnetic data used in this study. The authors also thank the ISGI (International Service of Geomagnetic Indices), GFZ German Research Centre for Geosciences, and the WDC (World Data Centre for Geomagnetism), Kyoto, Japan for geomagnetic indices data. Solar wind data were accessed through OMNIWeb, and we are thankful for their dataset.

5. References

Akasofu, S.I., 1981. Relationship between the AE and Dst indices during geomagnetic storms. *Journal of Geophysical Research*, **86**, 4820-4822. https://doi.org/10.1029/JA086iA06p04820

Baker, D.N., Kanekal, S.G., Li, X., Monk, S.P, Goldstein, J., and Burch, J., 2004. An extreme distortion of the Van Allen belt arising from the 'Hallowe'en' solar storm in 2003. *Nature*, **432**(7019), 878–881. https://doi.org/10.1038/nature03116

Bartels, J., Heck, N. H. and Johnston, H. F., 1939. The three-hour-range index measuring geomagnetic activity. *Terrestrial Magnetism and Atmospheric Electricity*, **44**(4), 411–454. https://doi.org/10.1029/TE044i004p00411

Collado-Villaverde, A., Muñoz, P., and Cid, C., 2024. Classifying and bounding geomagnetic storms based on the SYM-H and ASY-H indices. *Natural Hazards*, **120**,1141-1162. https://doi.org/10.1007/s11069-023-06241-1

Curto, J. J. and Marsal, S., 2007. Quality control of Ebro magnetic observatory using momentary values. *Earth Planets Space*, **59**, 1187–1196. https://doi.org/10.1186/BF03352066

Daglis, I.A. 2006. Ring Current Dynamics. In: Baker, D.N., Klecker, B., Schwartz, S.J., Schwenn, R., and Von Steiger, R. (eds) Solar Dynamics and Its Effects on the Heliosphere and Earth. Space Sciences Series of ISSI, **22**. Springer, New York, NY. https://doi.org/10.1007/978-0-387-69532-7_13

Dubyagin, S., Ganushkina, N., Kubyshkina, M., and Liemohn, M., 2014. Contribution from different current systems to SYM and ASY midlatitude indices, *Journal of Geophysical Research: Space Physics,* **119**(9), 7243–7263. https://doi.org/10.1002/2014JA020122

Foster, J. C., Erickson, P. J., Nishimura, Y., Zhang, S. R., Bush, D. C., Coster, A. J., et al., 2024. Imaging the May 2024 extreme aurora with ionospheric total electron content. *Geophysical Research Letters*, **51**, e2024GL111981. https://doi.org/10.1029/2024GL111981

Gillies, D.M., St.-Maurice J.P., McWilliams, K.A. and Milan, S., 2012. Global-scale observations of ionospheric convection variation in response to sudden increases in the solar wind dynamic pressure. *Journal of Geophysical Research*, **117**, A04209. https://doi.org/10.1029/2011JA017255

Gonzalez, W.D., Echer, E., Clua-Gonzalez, A.L. and Tsurutani, B.T., 2007. Interplanetary origin of intense geomagnetic storms (Dst < −100 nT) during solar cycle 23. *Geophysical Research Letters*, **34** (6), L06101. https://doi.org/10.1029/2006GL028879

Gosling, J.T., Bame, S.J., McComas, D.J. and Phillips, J.L., 1990. Coronal mass ejections and large geomagnetic storms. *Geophysical Research Letters,* **17** (7), 901-904. https://doi.org/10.1029/GL017i007p00901

Grandin, M., Bruus, E., Ledvina, V. E., Partamies, N., Barthelemy, M., Martinis, C., Dayton-Oxland, R., Gallardo-Lacourt, B., Nishimura, Y., Herlingshaw, K., Thomas, N., Karvinen, E., Lach, D., Spijkers, M., and Bergstrand, C., 2024. The geomagnetic superstorm of 10 May 2024: Citizen science observations, *EGUsphere [preprint]*, https://doi.org/10.5194/egusphere-2024-2174

Kwak, Y.S., Kim, J.H., Kim, S., Miyashita, Y., Yang, T., Park, S.-H., Lim, E.-K., Jung, J., Kam, H., Lee, J., et al., 2024. Observational Overview of the May 2024 G5-Level Geomagnetic Storm: From Solar Eruptions to Terrestrial Consequences, *Journal of Astronomy and Space Sciences*, **41** (3), 171–194. https://doi.org/10.5140/JASS.2024.41.3.171

Lakhina, G.S. and Tsurutani, B., 2016. Geomagnetic storms: Historical perspective to modern view. *Geoscience Letters*, **3,** 5. https://doi.org/10.1186/s40562-016-0037-4

Makarov, G.A., 2022. Geomagnetic indices ASY-H and SYM-H and their relation to interplanetary parameters. *Solar-Terrestrial Physics,* **8**(4), 36–43. https://doi.org/10.12737/stp-84202203

Parker, W. E. and Linares, R., 2024. Satellite Drag Analysis During the May 2024 Geomagnetic Storm. *Journal of Spacecraft and Rockets*, **61**(5). https://doi.org/10.2514/1.a36164

Schwenn, R., 2006. Space Weather: The Solar Perspective, *Living Reviews in Solar Physics,* **3**, 2. http://www.livingreviews.org/lrsp-2006-2

Singh, P., Sinha, A.K., Pathan, B.M. and Rawat, R., 2012. Solar flare effect on low latitude asymmetric indices, *J. Journal of Atmospheric and Solar-Terrestrial Physics,* **77**, 119-124. https://doi.org/10.1016/j.jastp.2011.12.010

Singh, R., Scipión, D.E., Kuyeng, K., Condor, P., De La Jara, C., Velasquez, J.P., Flores, R. and Ivan, E., 2024. Ionospheric disturbances observed over the Peruvian sector during the Mother's Day Storm (G5-level) on 10–12 May 2024. *Journal of Geophysical Research: Space Physics*, **129** (11), e2024JA033003. https://doi.org/10.1029/2024JA033003

Spogli, L., Alberti, T., Bagiacchi, P., Cafarella, L., Cesaroni, C., Cianchini, G., Coco, I., Di Mauro, D., Ghidoni, R., Giannattasio, F., Ippolito, A., Marcocci, C., Pezzopane, M., Pica, E., Pignalberi, A., Perrone, L., Romano, V., Sabbagh, D., Scotto, C., Spadoni, S., Tozzi, R. and Viola, M., 2024. The effects of the May 2024 Mother's Day superstorm over the Mediterranean sector: from data to public communication, *Annals of Geophysics*, **67**(2), PA218. https://doi.org/10.4401/ag-9117

Thomsen, M.F., 2004. Why Kp is such a good measure of magnetospheric convection. *Space Weather*, **2**(11), S11004

https://doi.org/10.1029/2004SW000089

Tulasi Ram, S., Veenadhari, B., Dimri, A. P., Bulusu, J., Bagiya, M., Gurubaran, S., et al., 2024. Super-intense geomagnetic storm on 10–11 May 2024: Possible mechanisms and impacts. *Space Weather*, **22** (12), e2024SW004126. https://doi.org/10.1029/2024SW004126

Watari, S., 2017. Geomagnetic storms of cycle 24 and their solar sources. *Earth, Planet and Space*, **69**, 70. https://doi.org/10.1186/s40623-017-0653-z

Wu, Y., Xu, W., Chen, G. et al., 2008. Ground magnetic characteristics of the storm-time ring current Asymmetry. *Science in China Series D: Earth Sciences,* **51**, 686–693. https://doi.org/10.1007/s11430-008-0045-0

Yamazaki, Y., Matzka, J., Stolle, C., Kervalishvili, G., Rauberg, J., Bronkalla, O., et al., 2022. Geomagnetic activity index Hpo. *Geophysical Research Letters*, **49** (10), e2022GL098860. https://doi.org/10.1029/2022GL098860

Yamazaki, Y., Matzka, J., Siqueira da Silva, M.V., Kervalishvili, G.N., Korte, M. and Rauberg, J., 2024. Assessment of Geomagnetic Activity for the Kp=9 “Gannon Storm” in May 2024 Based on Version 3.0 Hpo Indices. *ESS Open Archive*, http://dx.doi.org/10.22541/essoar.171838396.68563140/v1